JOURNAL OF CATALYSIS 112, 44–53 (1988)

Molybdenum Carbide Catalysts

II. Topotactic Synthesis of Unsupported Powders

J. S. LEE, L. VOLPE, F. H. RIBEIRO, AND M. BOUDART[1]

Department of Chemical Engineering, Stanford University, Stanford, California 94305

Received January 13, 1987; revised January 20, 1988

Metastable cubic α-MoC_{1-x} ($x \sim 0.5$) unsupported powders with specific surface area ca. 200 m^2 g^{-1} and particle size ca. 3 nm were prepared by temperature-programmed reaction (TPR) of MoO_3 with ammonia producing first Mo_2N which was subsequently converted to α-MoC_{1-x} by TPR with a CH_4/H_2 mixture. Alternatively, a direct TPR of MoO_3 with a CH_4/H_2 mixture also produced α-MoC_{1-x}, provided that a small amount of platinum was impregnated on MoO_3 prior to TPR. Reactions involved in both processes were topotactic, with formation of metastable α-MoC_{1-x} crystals exhibiting pseudomorphism with the original platelets of MoO_3, the starting material. Without platinum, the reaction between MoO_3 and CH_4/H_2 required a higher temperature of initial reduction and the reaction was not topotactic, leading to hexagonal Mo_2C, the thermodynamically stable phase of molybdenum carbide.

INTRODUCTION

A companion paper (*1*) described synthesis and catalytic properties of hexagonal Mo_2C unsupported powders with specific surface areas (S_g) of 50–100 m^2 g^{-1}. The synthesis involved temperature-programmed reaction (TPR) between MoO_3 of S_g (<1 m^2 g^{-1}) and a CH_4/H_2 mixture. These materials could be prepared in a single step without surface contamination by polymeric carbon. A surface completely covered with polymeric carbon could also be obtained with subsequent removal of the carbon by dihydrogen, thereby creating an active carbide surface.

Although these Mo_2C powders possess high values of S_g, higher values near 200 m^2 g^{-1} are desired with a corresponding particle size of ca. 3 nm. Indeed, the surface structure of metals varies greatly with particle size when the latter lies between 1 and 5 nm (*2*). Preparation of unsupported metallic molybdenum carbide with particle size less than 5 nm would provide an opportunity to study the effects of surface structure on a catalytic reaction without any metal–support interaction that can obscure the effect of particle size when observed for supported catalysts metals.

In previous studies at Stanford, Mo_2N with S_g greater than 200 m^2 g^{-1} was prepared by TPR up to 970 K between MoO_3 and ammonia (*3, 4*). The solid transformation of oxide-to-nitride was topotactic as {100} planes of Mo_2N were parallel to {010} planes of MoO_3. Further temperature-programmed carburization of this nitride led to a metastable face-centered cubic (FCC) carbide phase (*5*). This reaction is also topotactic in the sense that the FCC structure of the metal atoms remains unaltered. The product carbide retains the structure, crystalline size, and the high S_g of its nitride parent.

This paper is concerned with processes to synthesize cubic α-MoC_{1-x} unsupported powders with S_g greater than 200 m^2 g^{-1} by a novel topotactic reaction involving a direct coreduction/carburization of MoO_3 in the presence of platinum, also yielding α-MoC_{1-x} with the same high S_g. The synthe-

[1] To whom correspondence should be addressed.

0021-9517/88 $3.00

sized carbides are characterized by physical and chemical methods including X-ray diffraction (XRD), scanning electron microscopy (SEM), temperature-programmed reduction, and gas adsorption.

EXPERIMENTAL

High-purity MoO_3 powder (99.998%, Johnson-Matthey) was used as received to prepare nitride and carbide. Gases were purified according to the procedures described elsewhere (*1*). Also given were the description of the flow system for sample preparation and experimental procedures for gas adsorption, X-ray diffraction, and TPR.

A high-S_g nitride was prepared according to the procedure described previously (*4*). In the new procedure, platinum was introduced by incipient wetness impregnation of MoO_3 with a water solution of $H_2PtCl_6 \cdot 6H_2O$ such that the content of Pt after preparation was 0.25% by weight. The impregnated sample was dried at 350 K for 12 h in air. Carburization was accomplished by TPR of Mo_2N or MoO_3 impregnated with Pt (denoted by MoO_3/Pt henceforth) with 20% CH_4 in H_2 (denoted by CH_4/H_2 henceforth). The carburization of nitride was performed in the same reactor as that used for nitride preparation without exposure of nitride to air. A typical preparation employed 0.1–3.0 g of MoO_3 or MoO_3/Pt loaded on a coarse quartz fritted disk in the cell. Then a flow of 50–100 μmol s^{-1} of NH_3 or CH_4/H_2 at atmospheric pressure was initiated. The temperature of the sample was varied in a furnace coupled with controller/programmer and monitored locally with a thermocouple. The heating rate of TPR was typically 30 K h^{-1}, and the final temperature of preparation was 950–970 K. After preparation, the sample was quenched by removing the furnace and then isolated by stopcocks in order to transport the cell to the gas adsorption system. Figure 1 summarizes the

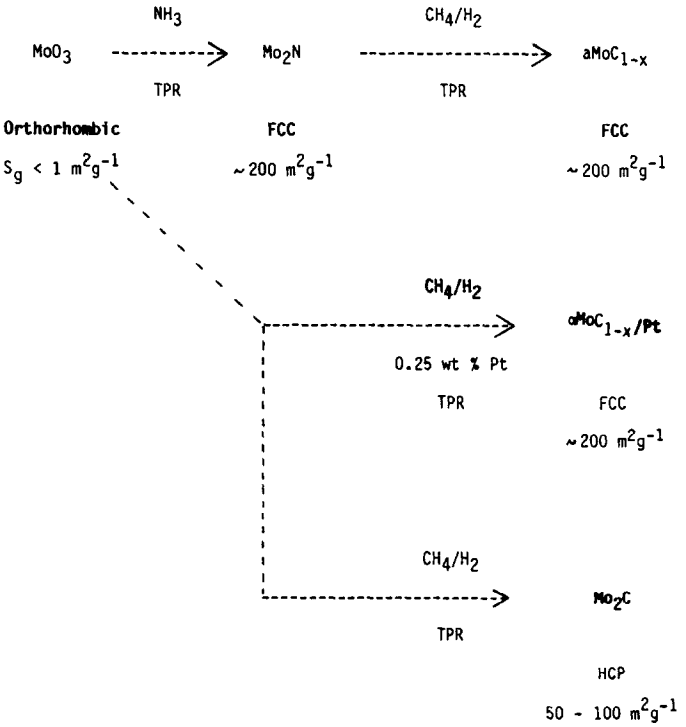

FIG. 1. Schematic procedures for synthesis of unsupported molybdenum carbide powders from MoO_3.

procedures to synthesize unsupported molybdenum carbide powders from MoO_3, their crystal structures, and S_g.

The carbide products were also characterized by temperature-programmed reduction in a mixture of 33% H_2 (Linde, prepurified) in He (Linde, high purity) flowing at a total rate of 20 μmol s^{-1}. Typically, 0.1 g of the carbide was heated from room temperature (RT) to 1370 K at a rate of 0.24 K s^{-1}. Before contacting the sample, the gas mixture passed through a molecular sieve trap at liquid nitrogen (LN_2) temperature and a MnO/SiO_2 indicator at RT. The reaction products were analyzed mass spectroscopically by a Hewlett–Packard 5970 mass selective detector. It was operated in the scanning mode with the data collected in steps of 0.125 m/e in the range 10–150 m/e, and a scan cycle time of ca. 1.5 s. The detection limit in the gas mixture was 1 ppm for CO and N_2 and 6 ppm for H_2O and CH_4. Calibration for CO, N_2, and CH_4 was made by sampling a known amount of these gases after each run.

For scanning electron microscopy (SEM), powder samples were dispersed on silver paint. An AMR 100 microscope was operated at 20 kV. Elemental analysis was performed in the Microanalysis Laboratory of the Department of Chemistry at Stanford University.

RESULTS

Preparation of Cubic α-MoC_{1-x} through Mo_2N Intermediates

In this preparation, a high-S_g Mo_2N reacted with a CH_4/H_2 mixture. The crystal structure of the product carbide was determined to be FCC by XRD with a lattice parameter 423 ± 1 pm. The molar ratio of C/Mo was determined to be ca. 0.5 by chemical analysis. Equilibrium isotherms of adsorption and desorption of N_2 measured at liquid nitrogen temperature are shown in Fig. 2. The abscissa P/P_0 represents a relative pressure, with P_0 being the saturation pressure of N_2 at LN_2 temperature. These isotherms can be viewed as a

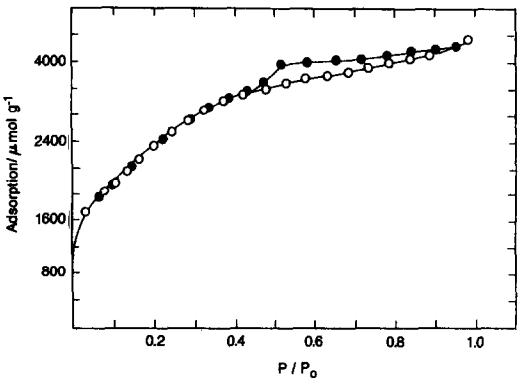

FIG. 2. Adsorption and desorption isotherms of N_2 on α-MoC_{1-x} at LN_2 temperature. (○) Adsorption isotherm. (●) Desorption isotherm.

combination of Types I and IV according to the classification of Brunauer *et al.* (*6*), and indicate that the sample contains both micropores with the half-width radius r_p of the pore less than 1 nm, and mesopores with r_p up to 30 nm. The shape of the adsorption–desorption hysteresis loop represents either slit-shaped pores or plate-like particles (*7*). Application of the standard BET method to adsorption data of $0.03 < P/P_0 < 0.25$ yielded the S_g of 205 m^2 g^{-1}. The characteristics of these isotherms are similar to those for the nitride precursor (*4*), suggesting that the carbide inherited the S_g, particle size, and pore structure of the parent nitride.

The gas products from the TPR between Mo_2N and CH_4 were monitored by a gas chromatograph, and the results are shown in Fig. 3. In this experiment, methane alone, instead of a 20% CH_4/H_2 mixture, was used as a carburizing gas in order to monitor H_2 produced from the reaction itself. Major events of transformation occurred around 800 and 940 K as indicated by coincident N_2 and H_2 peaks at these temperatures.

During the solid transformations of MoO_3 to Mo_2N, and then to α-MoC_{1-x}, the morphology of the solid did not alter. This pseudomorphism is demonstrated by SEM pictures of MoO_3, Mo_2N (*4*), and α-MoC_{1-x} in Fig. 4. All assume the highly anisotropic

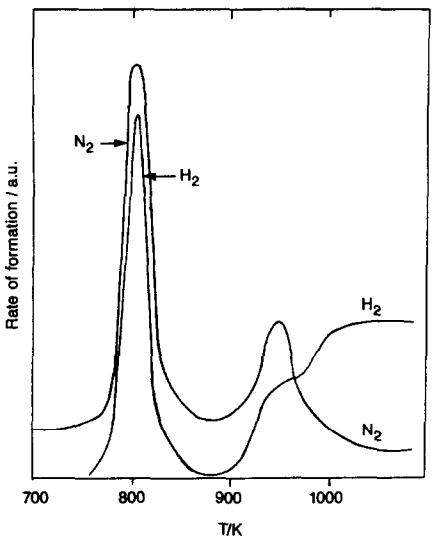

FIG. 3. Temperature-programmed reaction profiles for the transformation of Mo_2N to α-MoC_{1-x} by reaction with methane. The rate of heating was 30 K h^{-1}.

platelet shape. Meanwhile, Mo_2C prepared through a nontopotactic reaction path has no resemblance to MoO_3 in morphology as shown in Fig. 5.

In Table 1, powder XRD patterns of plate-like α-MoC_{1-x} in the present study are compared to those of α-MoC_{1-x} prepared from a sintered Mo_2N. The sintering involved heating the high-S_g Mo_2N powder at 1070 K in flowing N_2 for 12 h. This carbide had an S_g of 20 m^2 g^{-1}. The relative intensity of XRD peaks of the low-S_g α-MoC_{1-x} is very close to the theoretical intensity distribution for FCC crystal powders (*8*). The XRD pattern of high-S_g α-MoC_{1-x}, on the other hand, exhibits an extraordinarily high intensity of {h00} peaks.

Preparation of α-MoC_{1-x} by Direct Carburization of MoO_3 in the Presence of Platinum Catalyst

The MoO_3/Pt was heated in a CH_4/H_2 mixture in the same manner as that for the preparation of Mo_2C (*1*). Figure 6 shows a typical TPR profile of this synthesis process when a 20% CH_4/H_2 is used. The change in rates of methane consumption (Fig. 6a) and of water formation (Fig. 6b) was registered at linearly increasing temperatures. As compared to the synthesis of Mo_2C without a catalyst (*1*), two interesting features are noted. First, the presence of Pt greatly decreased the temperature for the early stage of reduction. The rate of water formation was appreciable from 400 K, much lower than uncatalytic reduction of MoO_3 which starts above 800 K (*1*). However, the same high temperature was required in both cases for a complete reduction/carburization. Second, unlike uncatalyzed reduction/carburization, methane was consumed even in the first stage of reduction.

The reduction in the presence of Pt started even at room temperature. Initially pale green MoO_3 powders slowly turned to black at room temperature in a flowing CH_4/H_2 mixture. The XRD pattern of this sample showed that molybdenum bronze H_xMoO_3 was formed (*9*). When TPR was halted at 500 K for the examination of the sample by XRD, a new intermediate was detected in addition to the previous molybdenum bronze. This intermediate had diffuse XRD peaks at $2\theta = 37.1°$ and 43.2° when Cu$K\alpha$ radiation was used as an X-ray source, with the latter peak in much higher intensity. The final product after TPR up to 950 K showed an XRD pattern of FCC crystal which was very similar to that of α-MoC_{1-x} prepared through the Mo_2N inter-

TABLE 1

Comparison of Cu$K\alpha$ Powder X-Ray Diffraction Patterns of High-S_g α-MoC_{1-x} with a Platelike Morphology and of Low-S_g α-MoC_{1-x}

2θ(°)	(hkl)	Relative intensity	
		High-S_g	Low-S_g
36.7	(111)	13	100
42.6	(200)	100	52
62.0	(220)	7	32
74.0	(311)	8	38
77.9	(222)	3	12
92.8	(400)	20	4

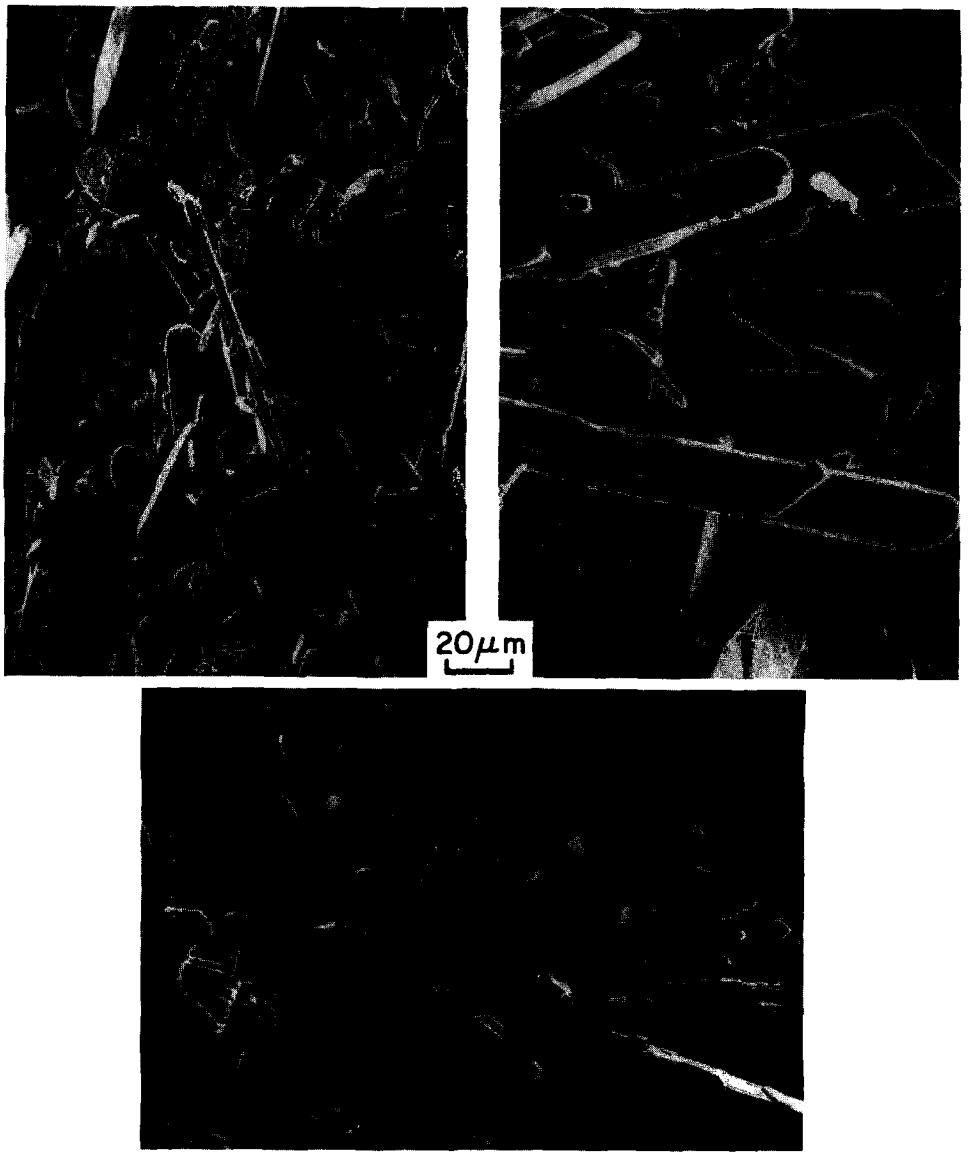

FIG. 4. Scanning electron micrographs showing pseudomorphism in the topotactic transformation of MoO_3 (left) to Mo_2N (right), and then to α-MoC_{1-x} (bottom).

mediate in both the positions and the relative intensity of peaks. The molar ratio of C/Mo prepared with a 20% CH_4/H_2 mixture was determined to be ca. 0.6 by chemical analysis.

The S_g of the final product depended on the composition of reacting gases as was the case with the synthesis of Mo_2C (*1*). The TPR with a 20% CH_4/H_2 mixture produced α-MoC_{1-x} with an S_g of 160 $m^2\ g^{-1}$. This carbide was dissolved in aqua regia without residue, indicating that there was no appreciable deposit of polymeric carbon on the surface (*5*). When an 80% CH_4/H_2 mixture was used, the product exhibited an S_g of 216 $m^2\ g^{-1}$ after H_2 treatment at 875 K to remove the polymeric carbon from the surface (*1*).

FIG. 5. Scanning electron micrograph of Mo_2C prepared by nontopotactic process. Note that the morphology of this carbide has no resemblance to its parent oxide.

Properties of Cubic α-MoC_{1-x} Powders

Table 2 shows the characterization data of two types of α-MoC_{1-x} and also of Mo_2C powders. The CO number density was calculated as the amount of irreversible CO uptake at room temperature per unit BET area. The particle sizes D_p were estimated from BET areas and the crystallite sizes D_c from application of the Scherrer equation to broadening of the X-ray diffraction peak width. Two types of α-MoC_{1-x} have very similar properties. Table 3 summarizes the structural differences between α-MoC_{1-x} and Mo_2C. As shown earlier, α-MoC_{1-x} inherits the platelet morphology of parent MoO_3 which is completely different from that of Mo_2C. Also, they have a different crystallographic arrangement of Mo atoms. However, both have very similar stoichiometry and first nearest-neighbor distances.

The temperature-programmed reduction of the fresh α-MoC_{1-x} powders in 33% H_2/He yielded data on sample purity, most importantly, the oxygen content. A typical temperature-programmed reduction profile

TABLE 2

Characterization Data of Unsupported Molybdenum Carbide Powders

	α-MoC_{1-x}	α-MoC_{1-x}/Pt	Mo_2C
S_g ($m^2\ g^{-1}$)	185	216	60
CO chemisorption ($\mu mol\ g^{-1}$)	800	805	218
CO number density ($10^{14}\ cm^{-2}$)	2.6	2.2	2.2
Particle size (nm)			
D_p by BET[a]	3.0	2.6	11.0
D_c by X-ray[b]	6.0	3.4	11.5

[a] $D_p = 6/\rho S_g$; ρ is the density; S_g is the specific surface area by BET.

[b] $D_c = \lambda/(\beta \cos \theta)$; λ is the wavelength of Cu$K\alpha$ X-ray radiation; θ is the Bragg angle; β is the half-width corrected for $K\alpha$-doublet separation and instrumental broadening.

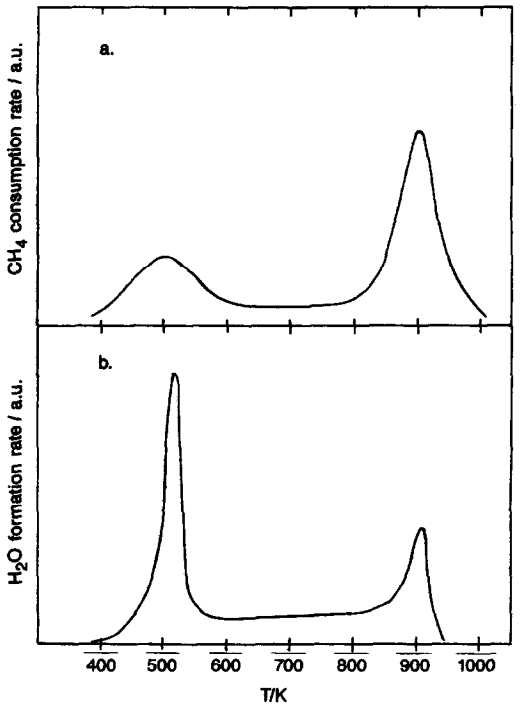

FIG. 6. Temperature-programmed reaction profiles for Pt-catalyzed reaction of MoO_3 with 20% CH_4/H_2 mixture. The rate of heating was 60 K h^{-1}. (a) Methane consumption rate. (b) Water formation rate.

is shown in Fig. 7. Only CH_4 and CO were detected.

At the end of the temperature programming the temperature was maintained at 1370 K for 1 h. During this treatment the rate of CH_4 and CO production stayed constant. The total amounts of CH_4 and CO for the α-MoC_{1-x} prepared from the nitride were, respectively, 4000 and 390 μmol g^{-1}, and for α-MoC_{1-x}/Pt 2100 and 270 μmol g^{-1}. Analysis of both samples by XRD after treatment revealed that the metastable cubic carbides were completely transformed to the thermodynamically stable hexagonal Mo_2C.

DISCUSSION

The phase diagram of the Mo–C system (*10*) indicates that only hexagonal Mo_2C is thermodynamically stable below 1940 K. This is the anticipated product under the conditions of our preparation. A cubic carbide α-MoC_{1-x} is metastable and could be obtained at low temperatures only by rapid quenching of Mo–C mixture from temperatures above 2235 K. This cubic carbide has been reported to have a lattice parameter a = 427–428 pm and a molar ratio of C/Mo from 0.65 to 0.75 (*10*). A smaller value of a of our carbide is probably due to a lower carbon content (*11*).

Oxygen remaining on a fresh carbide sample after preparation is a known impurity, particularly when an oxide is the precursor in the carbide preparation (*12*). As brought to the attention of the authors by a referee, the FCC α-MoC_{1-x} phase has an XRD pattern similar to that of the oxycar-

TABLE 3

Comparison of the Structure of α-MoC_{1-x} and Mo_2C

	α-MoC_{1-x}	Mo_2C
Morphology	Platelike	Random
Crystallographic arrangement of Mo atoms	FCC	HCP
Nearest neighbors		
Numbers		
Mo–C	3[a]	3
Mo–Mo	12	12
Distances (pm)		
Mo–C	212	209
Mo–Mo	299	296

[a] For x = 0.5.

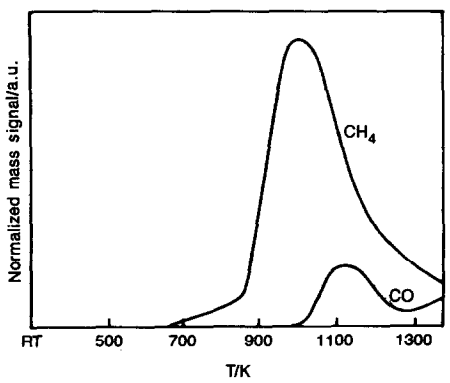

FIG. 7. Temperature-programmed reduction in 33% H_2/He of α-MoC_{1-x}.

bide. But there is no hexagonal-phase oxycarbide reported in the literature. When our FCC phases are transformed to the hexagonal Mo_2C in the temperature-programmed reduction experiments in 33% H_2/He, the amount of released CO corresponds to about 4 oxygen atoms for 100 molybdenum atoms. Based on this small oxygen content, we believe that our samples are not oxycarbides. The temperature-programmed reduction experiments are consistent with the $MoC_{0.6}$ stoichiometry given by the elemental analysis.

The two processes of preparation of cubic carbide described in the present paper involve the topotactic solid transformation because of the relationship of crystal structure between the parent and the product throughout the bulk of the solid (*13, 14*). Previously it was shown that {100} planes of Mo_2N and α-MoC_{1-x} were parallel to the {010} layers of MoO_3 (*4, 5*).

The nitride and the carbide, as products of topotactic reaction, exhibit pseudomorphism with their parent MoO_3, as shown by SEM pictures (Fig. 4). Both retain the external shape and dimensions of the particles of MoO_3, although the crystal structure, size, and density have been greatly changed from those of the oxide. The processes are illustrated schematically in Fig. 8. A platelet of single-crystal MoO_3 with dimensions of approximately 20 × 50 × 0.5 μm in the direction of [100], [001], and [010], respectively, exposes the extended (010) plane of orthorhombic unit cell. This converts to a platelet consisting now of many particles of Mo_2N or α-MoC_{1-x} of ca. 3 nm in size. A large decrease in specific volume and the formation of a large number of small particles are accompanied by development of internal pores which is responsible for the great increase in S_g. The platelet morphology would be uncharacteristic of cubic crystals like Mo_2N and α-MoC_{1-x}. It is simply inherited from parent MoO_3, the layered structure of which leads to platelet morphology.

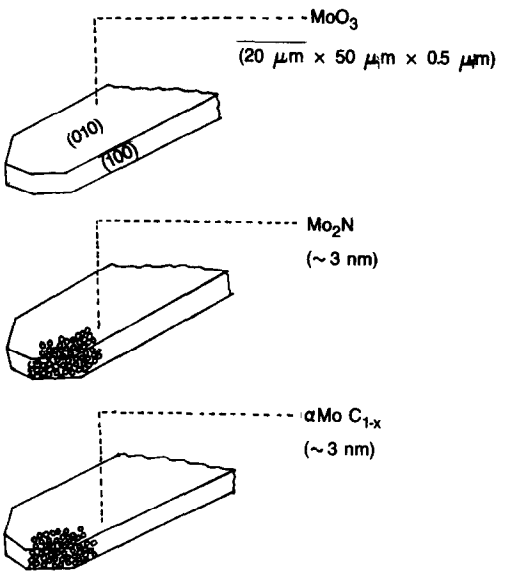

FIG. 8. Schematic illustration of the topotactic solid transformation of a platelet of MoO_3 to Mo_2N, and then to α-MoC_{1-x}. Although the shape and the size of the starting platelet are preserved in nitride and carbide, the size of the crystallite is greatly reduced and small pores are developed.

An ideal tool to identify topotaxy during a reaction of powdered solids is transmission electron microscopy (TEM) with selected area electron diffraction (SAD). The orientation relationship of lattices of MoO_3 and Mo_2N was examined with this technique (*3, 4*). The powder XRD ordinarily may not be used since the distribution of orientations of the crystallites masks the orientation correspondence between the diffracting planes of the parent and product crystals. For platelike particles, however, powder XRD has been successfully applied by Volpe and Boudart (*14*) to show that {100} planes of Mo_2N are parallel to the {010} layers of MoO_3. Likewise, the very high intensity of {100} peaks in the XRD pattern of platelike α-MoC_{1-x} in Table 1 shows that {100} planes of α-MoC_{1-x} are parallel to {100} planes of Mo_2N, and also to {010} layers of MoO_3. Since the relative intensity of XRD peaks of low-S_g α-MoC_{1-x} is similar to that of FCC powders, this sample seems to have assumed a random morphol-

ogy. Systematic abnormality in intensity distribution of powder XRD peaks thus indicates that topotactic reaction has occurred.

The formation of metastable phase, pseudomorphism, and systematic abnormality in intensity distribution of powder XRD peaks are all consequences of the topotactic nature of the nitride-to-carbide transformation. The solid transformation appears to involve movement of only nonmetal atoms. Thus N atoms diffuse out and C atoms move in to take their place while molybdenum atoms remain essentially motionless as their FCC structure stays unaltered.

The oxide-to-carbide transformation is much more complex than the apparently simple nitride-to-carbide transformation. It is well known that Group 8 metals catalyze the reduction of MoO_3 (*15–17*). The reaction of MoO_3/Pt with a CH_4/H_2 produces molybdenum bronze H_xMoO_3 even at room temperature. When MoO_3/Pt is brought into contact with dihydrogen, hydrogen atoms produced on Pt surface "spill over" to the oxide surface and further diffuse into the MoO_3 lattice, as is well documented by Fripiat (*18*). Upon further heating, water is produced and methane is consumed with the maximum rates at first at 520 K. This early stage of reaction produces a new intermediate. Previous studies of catalyzed reduction of MoO_3 in H_2 in the presence of Pd, Ni, and Re (*16, 17*) revealed that MoO_2 and other suboxides were formed at this stage, the XRD patterns of which are very different from that observed in the present study. In the synthesis of Mo_2C without a catalyst, on the other hand, the first methane consumption peak was absent (*1*). Thus it appears that methane dissociates on Pt producing carbon atoms which are subsequently incorporated into molybdenum oxide to form the oxycarbide intermediate. The XRD pattern of the intermediate could be assigned to be (111) and (200) peaks of MoO_xC_y, as for a FCC crystal known to be formed during the pyrolysis of $Mo(CO)_6$ (*19*). The formation of the oxycarbide intermediate is similar to the oxynitride formation that occurs during the MoO_3–NH_3 reaction (*4*).

The direct reduction/carburization of Pt-impregnated MoO_3 thus provides another topotactic route to prepare the cubic α-MoO_{1-x}. A topotactic reaction starts with oriented nucleation of product phase relative to the parent, and often leads to a metastable crystalline phase unattainable by other methods. The formation of metastable cubic carbide is a consequence of structural motives lying along the {010} layers of MoO_3, which are conserved during the solid transformations in the {100} planes of nitride or carbide. It is believed that the critical variable providing the topotactic reduction of MoO_3 is the low temperature at which the initial stage of reduction occurs. As in the case of the catalytic reduction with Pt, the reduction of MoO_3 with ammonia starts at a much lower temperature, around 620 K (*4*), than that for the uncatalyzed reduction by CH_4/H_2 where the water formation becomes noticeable above 800 K (*1*). Nucleation of the product phase presumably takes place during this initial stage of reduction. A low temperature at this stage would impose a restriction on atom displacement, leading to oriented nucleation of the product phase relative to the parent crystal.

ACKNOWLEDGMENTS

This work was initiated with support from NSF through the Center for Materials Research at Stanford University under the NSF-MRL Program. It has been completed with the help of DOE Grant DE-AT03-79ER10502-03. F. Ribeiro acknowledges CNPq Brazil for financial support.

REFERENCES

1. Lee, J. S., Oyama, S. T., and Boudart, M., *J. Catal.* **106,** 125 (1987).
2. Boudart, M., "Proceedings, 6th International Congress on Catalysis, London, 1976" (G. C. Bond, P. B. Wells, and F. C. Tompkins, Eds.), p. 1. The Chemical Society, London, 1976.

3. Volpe, L., Oyama, S. T., and Boudart, M., "Preparation of Catalysts III" (G. Poncelet and P. A. Jacobs, Eds.), p. 147. Elsevier, Amsterdam, 1983.
4. Volpe, L., and Boudart, M., *J. Solid State Chem.* **59,** 332 (1985).
5. Volpe, L., and Boudart, M., *J. Solid State Chem.* **59,** 348 (1985).
6. Brunauer, S., Demming, L. S., Demming, W. S., and Teller, E., *J. Amer. Chem. Soc.* **62,** 1723 (1940).
7. Gregg, S. J., and Sing, K. S. W., "Adsorption, Surface Area and Porosity," p. 111. Academic Press, London/New York, 1982.
8. Warren, B. F., "X-Ray Diffraction." Addison–Wesley, Reading, MA, 1969.
9. Birtill, J. J., and Dickens, P. G., *Mater. Res. Bull.* **13,** 311 (1978).
10. Rudy, E., Windisch, S., Stosick, A. J., and Hoffman, J. R., *Trans. TMS-AIME* **239,** 1247 (1967).
11. Storms, E. K., "Refractory Carbides," p. 132. Academic Press, New York, 1967.
12. Toth, L. E., "Transition Metal Carbides and Nitrides," p. 22. Academic Press, New York, 1971.
13. Oswald, H. R., and Gunter, J. R., "1976 Crystal Growth and Materials" (E. Kaldis and H. J. Scheel, Eds.), p. 416. North-Holland, Amsterdam, 1977.
14. Volpe, L., and Boudart, M., *Catal. Rev. Sci. Eng.* **27**(4), 515 (1985).
15. Hegedüs, A. J., Sasvari, K., and Neugebauer, J., *Z. Anorg. Allg. Chem.* **293,** 56 (1957).
16. Bond, G. C., and Tripathi, J. B. P., *J. Less-Common Met.* **36,** 31 (1974).
17. Grintsov, A. S., Skorokhod, V. V., Uvarova, I. V., and Solonin, Yu. M., *Russ. Metall.* **25,** 31 (1978).
18. Fripiat, J. J. "Surface Properties and Catalysis by Non-metals" (J. P. Bonnelle, B. Delmon, and E. Derouane, Eds.), p. 477. Dordrecht, 1983.
19. "Powder Diffraction File (Inorganic Compounds)" (W. F. McClune, Ed.), Pattern No. 17-104. JCPOS, Swarthmore, 1979.